

Reliability of Muscle Blood Flow and Oxygen Consumption Response from Exercise Using Near-infrared Spectroscopy

Adam A. Lucero¹, Gifty Addae², Wayne Lawrence², Beemnet Neway², Daniel P. Credeur³, James Faulkner⁴, David Rowlands¹, Lee Stoner^{1,5}.

¹*School of Sport & Exercise, Massey University, Wellington, New Zealand*, ²*School of Public Health, Harvard, Boston, MA, USA*. ³*School of Kinesiology, University of Southern Mississippi, MS., USA*, ⁴*Department of Sport and Exercise, University of Winchester, Winchester, United Kingdom*. ⁵*Department of Exercise and Sport Science, University of North Carolina at Chapel Hill, NC, USA*.

Running head: Local skeletal muscle blood flow and oxygen consumption assessment

Keywords: microvascular, hemodynamics, oxygen consumption

Word Count: 6287

Reference Count: 37

Subject Area: Human/environmental and exercise physiology

Correspondence:

Adam Lucero
School of Sport, Exercise, and Nutrition
Massey University
PO Box 756, Wellington
New Zealand
Adamluco1@gmail.com
ORCID: 0000-0002-2743-0209

This is the pre-peer reviewed version of the following article: Lucero et al. (2017). Reliability of Muscle Blood Flow and Oxygen Consumption Response from Exercise Using Near-infrared Spectroscopy. *Experimental Physiology*. – which has been published in final form at <https://doi.org/10.1113/EP086537>. This article may be used for non-commercial purposes in accordance with Wiley Terms and Conditions for Self-Archiving.

New Findings

- What is the central question of this study?

Continuous wave near-infrared spectroscopy coupled with venous and arterial occlusions offers an economical, non-invasive alternative to measuring skeletal muscle blood flow and oxygen consumption, however its reliability during exercise has not been established.

- What is the main finding and its importance?

Continuous wave near-infrared spectroscopy devices can reliably assess local skeletal muscle blood flow and oxygen consumption from the vastus lateralis in healthy, physically active adults. The patterns of response exhibited during exercise of varying intensity agree with other published results using similar methodologies, meriting potential applications in clinical diagnosis and therapeutic assessment.

Abstract

Near-infrared spectroscopy (NIRS), coupled with rapid venous (VO) and arterial occlusions (AO) can be used to non-invasively estimate resting local skeletal muscle blood flow (mBF) and oxygen consumption ($m\dot{V}O_2$), respectively. However, the day-to-day reliability of mBF and $m\dot{V}O_2$ responses to stressors such as incremental dynamic exercise has not been established. *Purpose:* To determine the reliability of NIRS derived mBF and $m\dot{V}O_2$ response from incremental dynamic exercise. *Methods:* Measurements of mBF and $m\dot{V}O_2$ were collected in the *vastus lateralis* of twelve healthy, physically active adults [7 m and 5 f; 25 y (SD 6)] over 3 non-consecutive visits within 10 days. After 10 mins rest, participants performed 3 mins of rhythmic isotonic knee extension (1 extension/4 s) at 5, 10, 15, 20, 25, and 30% of maximal voluntary contraction (MVC), prior to 4 VOs and then 2 AOs. *Results:* mBF and $m\dot{V}O_2$ proportionally increased with intensity (0.55 to 7.68 $\text{ml}\cdot\text{min}^{-1}\cdot 100\text{ml}^{-1}$ and 0.05 to 1.86 $\text{mlO}_2\cdot\text{min}^{-1}\cdot 100\text{g}^{-1}$, respectively) up to 25% MVC where it began to plateau at 30% MVC. Moreover, a mBF/ $m\dot{V}O_2$ ratio of ~ 5 was consistent for all exercise stages. The intra-class coefficient (ICC) for mBF indicated high to very high reliability for 10-30% MVC (0.82-0.9). There was very high reliability for $m\dot{V}O_2$ across all exercise stages (ICC 0.91-0.96). *Conclusion:* NIRS can reliably assess muscle blood flow and oxygen consumption responses to low-moderate exercise, meriting potential applications in clinical diagnosis and therapeutic assessment.

1 **Introduction**

2 Advancements in apparatuses and methods have permitted measurement and enhanced
3 understanding of *in vivo* local skeletal muscle blood flow (mBF) (Rådegran, 1999; Casey *et al.*,
4 2008). Using techniques such as magnetic resonance imaging, contrast enhanced ultrasound, and
5 intravascular tracer injection, the kinetics of flow through the microvasculature have been found
6 to act differently of bulk flow through large conduit vessels (Vincent *et al.*, 2002), hence bulk
7 flow may not accurately represent mBF (Harper *et al.*, 2006), the site of gas exchange, nutrient,
8 and hormone delivery. In addition, mBF can vary throughout a single muscle (Quaresima *et al.*,
9 2004) and is tightly matched to metabolic demand (Joyner & Casey, 2015). Skeletal muscle
10 oxygen consumption ($m\dot{V}O_2$) may be an important factor driving the regulation of mBF with
11 previous evidence showing that $m\dot{V}O_2/mBF$ ratio is maintained at a ratio of ~ 0.1 at rest and
12 during exercise in healthy individuals (Vogiatzis *et al.*, 2015).

13 Characterizing mBF and $m\dot{V}O_2$ at rest and during dynamic exercise has become an
14 important component of skeletal muscle hemodynamic and metabolic assessment and is
15 necessary to fully comprehend blood flow regulation and dysregulation in humans. However,
16 assessment of mBF during exercise is limited due to apparatus design, cost, technical skill,
17 invasiveness, and functionality with various populations (Andersen *et al.*, 1985; Paunescu *et al.*,
18 1999; Rådegran, 1999; Casey *et al.*, 2008; Rudroff *et al.*, 2014). There exists a need for a
19 reliable, non-invasive, and affordable technique that can effectively investigate mBF and $m\dot{V}O_2$
20 kinetics in various populations and disease states under real-world exercise conditions.

21 Continuous wave near-infrared spectroscopy (NIRS) is an emerging, affordable, and
22 portable technology which enables the assessment of skeletal muscle hemodynamics through
23 relative concentrations of oxygenated and deoxygenated hemoglobin. Currently, NIRS cannot

24 differentiate between hemoglobin and myoglobin, but its contribution to the NIR signal is
25 suggested to be less than 20% at rest, with the main contributor being hemoglobin (Ferrari *et al.*,
26 2011). Given that NIRS only measures changes in vessels smaller than 1-2 mm in diameter, it is
27 ideal for assessing local skeletal muscle microcirculation (Mancini *et al.*, 1994). Combining
28 NIRS with rapid venous (VO) and arterial (AO) occlusions to estimate mBF and $m\dot{V}O_2$,
29 respectively, has been validated in the forearm (Van Beekvelt *et al.*, 2001; Cross & Sabapathy,
30 2015), calf (Casavola *et al.*, 2000), and VL (Quaresima *et al.*, 2004). However, this technique
31 has been limited to rest and maximal isometric exercise states and no protocol has been
32 developed to reliably assess both mBF and $m\dot{V}O_2$ response to specific steady state exercise. The
33 purpose of this study was to determine the reliability of continuous wave NIRS derived estimates
34 of mBF and $m\dot{V}O_2$ in the *vastus lateralis* (VL) in response to incremental dynamic knee
35 extension exercise.

36 **Methods**

37 *Ethical Approval*

38 Twelve healthy, (7 males and 5 females) physically active (>3 h of moderate intensity
39 exercise per week) adults participated in this study (Table 1). Participants were excluded if they
40 were smokers, reported any known cardio-metabolic disorders, or were taking medications
41 known to affect cardiovascular function. This study was not designed to examine potential sex
42 differences; thus, menstrual cycle status was not controlled for in female participants. Ethical
43 approval was obtained from the institutional Human Ethics Committee (HEC: Southern A
44 Application) and in accordance with the 1964 Helsinki declaration and its later amendments or
45 comparable ethical standard, except for registration in a database. All participants were informed

46 of any risks and discomfort associated with the experiments prior to providing written informed
47 consent.

48 *Experimental Procedures*

49 Each participant was tested on four different days in a dimly-lit, temperature controlled
50 room [(20.5 °C (SD 0.8)]. On visit 1, participants were familiarized with the testing protocol and
51 their maximum voluntary contraction (MVC) for a 90° isometric knee extension was obtained
52 and reported as the maximum of three trials using an isokinetic dynamometer (Biodex Medical
53 Systems, Inc. Shirley, NY, USA). To determine the MVC, the participant was seated on the
54 dynamometer reclined to 70° giving a 110° hip angle, and the settings were adjusted so that the
55 axial portion of the knee aligned with the axis of rotation on the dynamometer. When assessing
56 mBF and $m\dot{V}O_2$, the participant's dominant leg was suspended at a 'neutral' position during
57 occlusion. The 'neutral' position consisted of a knee-joint angle of 150° , which permitted a
58 relaxed muscle length, thereby facilitating blood flow (Miura *et al.*, 2004). The non-working leg
59 was suspended in neutral position throughout.

60 The experimental protocol was conducted on visits 2-4. All experimental tests occurred
61 between the hours of 7-10 am following an overnight fast, having consumed only water,
62 refraining from caffeine and supplement intake that morning. Participants also avoided strenuous
63 physical activity and alcohol for 24 hours prior to experimentation. Using hemoglobin as an
64 endogenous intravascular tracer, venous and arterial occlusions were used to estimate mBF and
65 $m\dot{V}O_2$. Participants were seated on the dynamometer and while the NIRS probe was adhered to
66 the skin and cuff was placed and tested for positioning and comfort. Following an additional 10
67 min of quiet seated rest, baseline measurements of mBF and $m\dot{V}O_2$ were assessed as the average
68 of 4 VO and 2 AO measurements, respectively. Each occlusion was separated by 45 s of rest

69 with VO durations of 15 s and AO durations of 15 and 30 s (Southern *et al.*, 2013). The
70 participant then completed 6 stages of progressive intensity (5, 10, 15, 20, 25, and 30% of MVC)
71 90° rhythmic isotonic knee extension exercise (1 extension/4 sec) on the dynamometer
72 (Watanabe & Akima, 2011).

73 For each intensity, the participant exercised continuously for 3 min prior to occlusions.
74 This time was chosen as a balance between the likelihood of achieving steady state physiology
75 without causing fatigue. Steady state was determined through pilot trials by a stabilizing of
76 whole body oxygen consumption. Participants were instructed to contract to full extension and
77 then allow their leg to fall back to the starting position. Immediately after the contraction phase
78 of the last knee extension for each measurement point, as the leg was falling, the dynamometer
79 was locked to hold the leg in the neutral position simultaneously as the cuff was inflated for 10 s.
80 This caused a brief pause in exercise during which the occlusion occurred. Exercise was then
81 resumed for 45 s to maintain steady state before another measurement was collected. As with
82 baseline measurements, mBF and $m\dot{V}O_2$ were assessed as the average of 4 VO and 2 AO
83 measurements, respectively (see Fig. 1A). Complete occlusion during AO at rest and exercise
84 was verified with Doppler ultrasound in the femoral artery during pilot trials and confirmed
85 during testing by the cessation of the pulsatile motion in the tHb signal. An index of perfusion
86 change and tissue saturation index were also assessed during each stage.

87 *Near-infrared Spectroscopy*

88 A continuous wave NIRS device (PortaLite, Artinis Medical Systems BV, the
89 Netherlands) emitted wavelengths of 760 and 850 nm to detect relative changes in concentrations
90 of oxygenated hemoglobin [HbO₂] and deoxygenated hemoglobin [HHb], respectively, as well
91 as total blood volume ([tHb] = [O₂Hb] + [HHb]). Absolute hemoglobin concentrations can be

92 estimated, however, in this study only relative changes are used in calculations. Wavelengths
93 were emitted from LEDs with an inter-optode distances of 3.5 cm, allowing for theoretical
94 penetration distances of 1.75 cm (Chance *et al.*, 1992). A differential path-length factor of 4.0
95 was used to correct for photon scattering within the tissue, and data were collected at 10 Hz
96 (Oxysoft, Artinis Medical Systems BV, the Netherlands). The NIRS probe was securely adhered
97 to the skin parallel to the muscle fibers, about two-thirds from the top of the *vastus lateralis* over
98 the muscle belly. A custom-made cover shielded the probe from ambient light while allowing it
99 to move with the skin during contractions minimizing changes in contact pressure (Hamaoka *et*
100 *al.*, 2011). The thickness of the muscle at this location, along with adipose tissue thickness, was
101 determined using B-mode ultrasound (Terason, United Medical Instruments Inc., San Jose, CA,
102 USA).

103 *Local Skeletal Muscle Blood Flow*

104 Estimates of mBF were assessed as the $[\Delta\text{tHb}]$ signal during VO, analyzed using simple
105 linear regression as previously described (Van Beekvelt *et al.*, 2001; Cross & Sabapathy, 2015).
106 Briefly, a tourniquet (Hokanson SC 10D, D. E. Hokanson, Inc., Bellevue, WA, USA) was placed
107 as high as possible around the proximal thigh, minimizing patient discomfort and avoiding
108 artefact motion in the NIRS signal. The tourniquet was rapidly (~ 0.5 s) inflated to a subdiastolic
109 pressure (60-80 mmHg) occluding venous outflow without impeding arterial inflow, thus,
110 causing venous volume to increase at a rate proportional to arterial inflow (Van Beekvelt *et al.*,
111 2001). After cuff inflation, there is a rapid, progressive fall in the rate of $[\Delta\text{tHb}]$ (especially
112 during exercise), likely due to an increase in venous backpressure, diminishing the arteriovenous
113 pressure gradient and stimulating the venoarterial reflex causing vasoconstriction of precapillary
114 vessels (Rathbun *et al.*, 2008). As a consequence, inclusion of more than one cardiac beat has

115 been shown to underestimate mBF (Cross & Sabapathy, 2015) (see Fig. 1B, C). Therefore,
 116 estimates of mBF were over the first cardiac cycle, defined using the pulsatile motion of the
 117 [tHb] signal. The slope of the [tHb] signal for each VO was averaged and converted into units of
 118 mL per min per 100 mL of blood ($mBF (mL \cdot min^{-1} \cdot 100 mL^{-1}) = 1/C \cdot [\Delta tHb]/\Delta t$) where
 119 $[\Delta tHb]/\Delta t$ is the average rate of tHb increase under VO (μM of Hb $\cdot s^{-1}$) and C is hemoglobin
 120 concentration in the blood, for which we assumed a value of 7.5 and 8.5 $mmol \cdot L^{-1}$ for female and
 121 male participants, respectively (Van Beekvelt *et al.*, 2001). The molecular mass of hemoglobin
 122 ($64.458 g \cdot mol^{-1}$) and the ratio between hemoglobin and O_2 molecules (1:4) were accounted for.

123 *Skeletal Muscle Oxygen Consumption*

124 Estimates of $m\dot{V}O_2$ were calculated as the rate of change in the Hb difference signal
 125 ($[\Delta HbDif] = [\Delta HbO_2] - [\Delta HHb]$) during arterial occlusion (see Fig. 1D,E), analyzed using
 126 simple linear regression as previously described (Ryan *et al.*, 2012). Briefly, the tourniquet was
 127 rapidly (~ 0.5 s) inflated to a supra-systolic pressure (250-300 mmHg) to occlude both venous
 128 outflow and arterial inflow, completely arresting blood flow, resulting in an increase of [HHb]
 129 and simultaneous decrease in [HbO₂] as oxygen is released from hemoglobin and consumed by
 130 the surrounding muscle tissue (Van Beekvelt *et al.*, 2001). After correcting for blood-volume
 131 changes (Ryan *et al.*, 2012), the slope of the [HbDif] signal for both AOs was averaged and
 132 converted into milliliters of O_2 per min per 100 grams of tissue ($m\dot{V}O_2 (mLO_2 \cdot min^{-1} \cdot 100g^{-1}) =$
 133 $abs([\Delta HbDif/2] \cdot 60) / (10 \cdot 1.04) \cdot 4 \cdot 22.4/1000$), assuming 22.4 L for the volume of gas (STPD)
 134 and $1.04 kg \cdot L^{-1}$ for muscle density (Van Beekvelt *et al.*, 2001).

135 *Local Skeletal Muscle Perfusion Change and Tissue Saturation Index*

136 An estimate of relative local skeletal muscle perfusion was calculated as the relative
 137 average blood volume ([tHb] signal) for a given period. The [tHb] signal has been said to reflect

138 microvascular blood-volume (Ijichi *et al.*, 2005) which reflects local O₂ diffusing capacity
139 (Groebe & Thews, 1990). Since the [tHb] signal measures absolute changes from a set baseline,
140 the resting value was set to 0 and the workload values were calculated as μM increases from rest.
141 The tissue saturation index (TSI%) was calculated with manufacturer software using a spatially-
142 resolved spectroscopy approach. The TSI% signal was averaged over the same period used for
143 perfusion analysis.

144 After resting measurements of mBF and $m\dot{V}\text{O}_2$ were taken, the participant's leg was
145 lowered to 90° knee-joint angle in preparation for the exercise protocol. The participant then
146 continued to rest to allow the [tHb] signal to stabilize for 30 s to assess resting perfusion and
147 TSI%. Estimated relative perfusion and TSI% were assessed as the average [tHb] and TSI%
148 signal during the 2 s rest period between knee extensions (when the leg was relaxed at 90°) of the
149 last 8 extensions before the first VO.

150 *Electromyography, Whole Body Oxygen Consumption & Heart Rate*

151 To verify the exercise model elicited the desired metabolic increases, in a separate testing
152 session surface electromyography (EMG), whole body oxygen consumption ($\dot{V}\text{O}_2$), and heart
153 rate (HR) were measured in a subset of individuals (N=7). The EMG electrode (Telemetry DTS,
154 Noraxon Inc., Scottsdale, AZ, USA) was placed over the NIRS probe location. To normalize the
155 EMG activity signal prior to beginning the exercise protocol, the participant performed 3 MVCs
156 and the peak forces were averaged and set to 100% activation. Integrated raw EMG signals were
157 analyzed according to standard methods for knee extension exercise (Alkner *et al.*, 2000). To
158 measure $\dot{V}\text{O}_2$, a breath-by-breath automatic gas exchange system (Vmax Spectra 29c,
159 SensorMedics Corporation, Yorba Linda, CA, USA) was used, and HR was monitored using a
160 wireless chest strap telemetry system (Polar Electro T31, Kempele, Finland).

161 Resting and exercise stage protocols were conducted like visits 2-4. However, during
162 exercise after the first three minutes of knee extensions, the leg was not rested as occlusions were
163 not required for assessing parameters. Baseline measures were assessed as the average value for
164 the last minute of the resting period. Exercise parameters were assessed during the fourth minute
165 of exercise. Exercise EMG activity was assessed as the average rectified maximum activity for
166 the last eight contractions for each stage. Exercise $\dot{V}O_2$ and HR data were expressed as the
167 average value for the last 60 seconds (fourth minute) of each stage.

168 *Statistical Analysis*

169 Statistical analyses were performed using Statistical Package for Social Sciences version
170 21 (SPSS, Inc., Chicago, Illinois). All data are reported as means with 90% confidence intervals,
171 unless otherwise specified. The NIRS parameters were analyzed to test the effects of intensity
172 and visit order using a two-way repeated measures analysis of variance (ANOVA)...
173 Mechanistic inference testing for substantial differences between intensities were calculated
174 from a published spreadsheet using generated p-values (Hopkins, 2007), with likelihood
175 thresholds of 50% (possible), 75% (likely), 95% (very likely), and 99% (most likely) chance of
176 substantial change. Values for mBF as a function of $m\dot{V}O_2$ were assessed for linearity using
177 linear regression to test goodness of fit as a coefficient of determination (R^2). Likelihoods for
178 correlations using magnitude based inference was used to test individual parameters against
179 exercise intensity and to each other using 95% confidence limits with 0.2 as the threshold for
180 smallest magnitude threshold for differences or change scores (Hopkins, 2007).

181 Reliability statistics were calculated with the log transformed raw data using published
182 spreadsheets (Hopkins, 2015) as described previously (Hopkins *et al.*, 2009). The typical error
183 (i.e. standard error of measurement) defined as $SD/\sqrt{2}$ where SD is the standard deviation of the

184 change score for all participants. Test-retest reliability statistics calculated include the intra-class
185 correlation coefficient (ICC), standardized typical error (STE), percentage coefficient of
186 variation (%CV) and percentage of the smallest effect (%SE). The ICC gives visit to visit
187 reproducibility for a given intensity and was calculated as $1-sd^2/SD_b^2$ where the *sd* is the typical
188 error and *SD_b* the mean between-participant standard deviation. Thresholds of 0.20 (low), 0.50
189 (moderate), 0.75 (high), 0.90 (very high), and 0.99 (nearly perfect) reliability for sample
190 populations were used. The STE gives the random error in the calibrated value and is interpreted
191 using thresholds of 0.1 (small), 0.3 (moderate), 0.6 (large), 1 (very large), and 2 (extremely
192 large) (Hopkins *et al.*, 2009). The typical error as a percentage is shown as CV (%). The SE (%)
193 represents the percentage above or below the measured value required for the smallest
194 worthwhile effect given by $0.2 \cdot SD_p$ where the *SD_p* is the pure between-subject standard deviation
195 calculated as above.

196 **Results**

197 Mean values and inferences for mBF and $m\dot{V}O_2$, relative perfusion, and TSI% are shown
198 in Fig. 2. Mean values for mBF and $m\dot{V}O_2$ were most likely (i.e., 99% chance) substantially
199 greater than resting across all intensities. For both mBF and $m\dot{V}O_2$, mean values for all
200 intensities were substantially greater than the previous intensity except for 30% MVC. Mean
201 mBF correlated linearly with exercise intensity, and was directly proportional to $m\dot{V}O_2$ ($y =$
202 $3.75x + 0.5384$; $R^2 = 0.8195 - 0.9814$ (Fig. 3A). The mean $m\dot{V}O_2/mBF$ ratio was 0.045 at rest
203 and varied from 0.104-0.132 for all exercise stages (Fig. 3B). Mean values for perfusion change
204 from rest at 15-30% MVC were substantially greater to resting, however, only trivial increases to
205 the previous intensity were seen in 10-30% MVC. Mean values for TSI% at 5, 10, and 30%
206 MVC were substantially less than resting. Mean values for EMG, $\dot{V}O_2$, and HR during exercise

Local skeletal muscle blood flow and oxygen consumption assessment
increased substantially from resting (Fig. 4). For all three parameters, no substantial increase was
observed at 10 and 25% MVC from the previous exercise intensity. There was a likely
substantial increase in HR at 30% MVC, but not in EMG and $\dot{V}O_2$. All seven parameters were
most likely substantially correlated with % MVC and to each other (99.7%-100% likelihood). No
visit order effect was observed for all NIRS parameters.

Reproducibility for all NIRS parameters is shown in Table 2 as statistic value, with
upper and lower 90% confidence limits available as supporting information. For mBF, the ICC
indicated moderate reliability (0.69) at 5% MVC, but high reliability at rest and across all other
intensities (0.82-0.89) with very high reliability at 25% MVC (0.9). The STE was moderate for
rest and all exercise stages (0.35-0.59). It was lowest (best) for 20 and 25% MVC (0.37 and 0.35,
respectively) and highest (worst) for 5 % MVC (0.59). The CV varied from 20.2 – 31% and was
lowest (best) for 10-25% MVC (20.9-24.8%). The SE varied from 5.5-10.2%. For $m\dot{V}O_2$ the ICC
indicated moderate reliability at rest (0.58) and very high reliability across all exercise stages
(0.91-0.96). The STE was moderate at rest (0.58) and 5-20% MVC (0.31-0.34), and low (best)
for both 25 and 30% MVC (0.22). The CV was 50.4% at rest, 20-22.6% for 5-20% MVC, and
13.5-14.0% for 25-30% MVC. The SE varied from 9.2-13.3% for all exercise stages.

Discussion

The purpose of this study was to determine the reliability of continuous wave NIRS
derived estimates of mBF and $m\dot{V}O_2$ in the *vastus lateralis* during short intermittent pauses from
dynamic exercise. Using occlusion methodology (i.e. AO and VO) combined with isotonic knee
extensions at specific intensities, according to the ICC values, the current study found high to
very high reliability from 10-30% MVC, and moderate reliability at 5% MVC. Comparing
absolute estimates of mBF and $m\dot{V}O_2$ with previously reported values is difficult due to

230 differences in exercise modality, muscle groups measured, and units used to express values.
231 However, patterns of response in mBF and $m\dot{V}O_2$ to exercise intensity are in agreement with
232 established results (Joyner & Casey, 2015), and the $m\dot{V}O_2/mBF$ ratio is also consistent with
233 previous findings (Vogiatzis *et al.*, 2015). Compared to other techniques, NIRS offers reliable,
234 non-invasive application to real-world exercise modalities, and can be used on a wide variety of
235 clinical populations (Paunescu *et al.*, 1999; Rådegran, 1999).

236 The relationship between mBF and $m\dot{V}O_2$ was consistent for all exercise intensities and
237 within range of published mBF/ $m\dot{V}O_2$ ratios of ~ 5 (Whipp & Ward, 1982; Richardson *et al.*,
238 1995; Kalliokoski *et al.*, 2005), showing a tight match of mBF to $m\dot{V}O_2$ during steady-state
239 exercise. For both mBF and $m\dot{V}O_2$, no substantial increase was seen from 25-30% MVC, as well
240 as 20-30% MVC for EMG activity and $\dot{V}O_2$. Taken together, the current results suggest that
241 maximal recruitment and/or fatigue developed in the primary *vastus lateralis* muscle fibers
242 prompting recruitment of accessory and additional muscle fibers in the quadriceps to sustain
243 contractions (Komi & Tesch, 1979; Vøllestad, 1997). In support, many participants [N=8]
244 appeared to have greater *rectus femoris* use at the higher intensities. Therefore, to obtain more
245 accurate steady state estimates of mBF and $m\dot{V}O_2$ at specific intensities, it is recommended that
246 in future trials, only 2 workloads between 10-25% MVC be tested in succession with adequate
247 rest in between, depending on the population being tested. For example, 15 and 25% MVC may
248 be ideal for physically active to athletic populations, but future trials will be needed to
249 characterize intensities that can be maintained in clinical populations while achieving
250 reproducible results.

251 Comparing the absolute estimates of mBF to those from other studies is difficult because
252 a) mBF is heterogeneous across the muscle and can vary widely depending on the region

253 measured, b) exercise modality used, and c) the units used to report mBF. Using a similar VO
254 technique with a frequency-domain NIRS device, Quaresima *et al.* (2004) estimated blood flow
255 to increase from 0.3-0.5 mL·min⁻¹·100 mL⁻¹ to 1.4-2.1 mL·min⁻¹·100 mL⁻¹ across the *vastus*
256 *lateralis* from rest to maximal isometric exercise. Although the exercise modality differs to the
257 current study, the resting value is within range of the current study and the exercise value for
258 maximal isometric contraction is lower. Comparing indocyanine green injection and ¹³³Xe,
259 Boushel *et al.* (2000) measured regional mBF in the calf during incremental plantar-flexion
260 exercise to 9 watts, and found similar mBF values between the techniques concluding that mBF
261 rose from about 2.2 mL·min⁻¹·100 mL⁻¹ to 15.1 mL·min⁻¹·100 mL⁻¹. Although these estimates
262 are larger than those reported in the current study, the muscle group and exercise modality differ.
263 However, like the current study, the authors found increases in mBF to be proportional to
264 workload.

265 Using thermodilution and dynamic knee extension exercise at 60 rpm to peak power,
266 Rådegran *et al.* (Rådegran *et al.*, 1999) found peak knee extensor mBF and m $\dot{V}O_2$ to be 246.2 ±
267 24.2 mL·min⁻¹·100 g⁻¹ and 34.9 ± 3.7 mL·min⁻¹·100 g⁻¹, respectively, which is substantially
268 higher than the current study. However, the exercise modalities differed significantly, in that the
269 current study only went to 30% MVC, allowed for greater rest between contractions, and the
270 force was only exerted at 90° rather than throughout extension, which would isolate a lower mass
271 of contracting muscle (Joyner & Casey, 2015). Moreover, the current study measured one region
272 within one knee extensor, the *vastus lateralis*, which has been shown exhibit ~57% mBF
273 heterogeneity and to have ~20% less blood flow than the *vastus intermedius* during knee
274 extension exercise (Rudroff *et al.*, 2014). In the previous study, using positron emission
275 tomography, the authors found mBF in the *vastus lateralis* to be 6.21 ± 1.96 and 9.77 ± 3.82
276 mL·min⁻¹·100 g⁻¹ at 2 and 12 min, respectively, of sustained isometric contraction at 25% MVC

Local skeletal muscle blood flow and oxygen consumption assessment
277 in young men, which is within range of the current study. In addition, EMG activity was also
278 within range of the current study.

279 **Limitations and Future Direction**

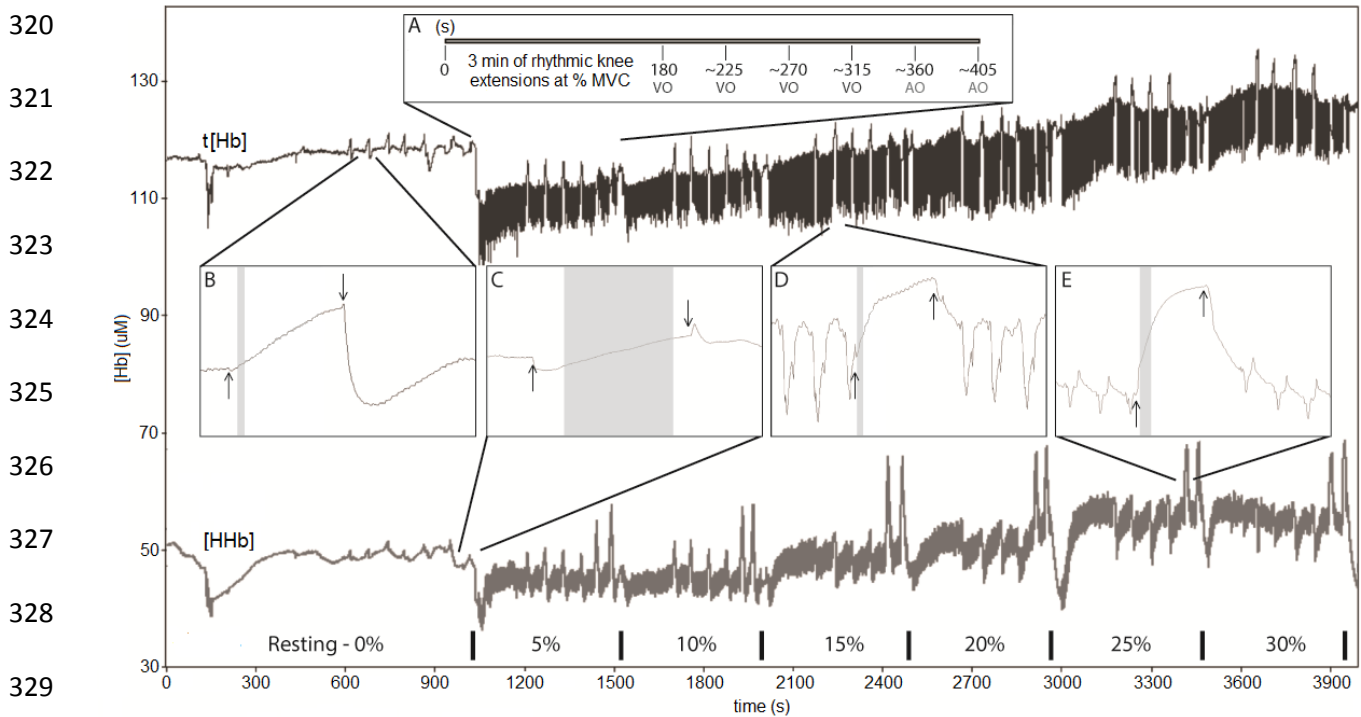
280 Future application of the current protocol should consider a) timing of cuff inflation, b)
281 addition of ECG monitoring and individual blood sampling, and c) concurrent monitoring of
282 additional non-invasive measurements for assessing the entire oxygen cascade. Firstly, since VO
283 can only be inflated between contractions, the resulting tHb slope reflects post-contraction values
284 and not exercise *per se* (Rådegran, 1999). However, immediate post-exercise mBF has been
285 shown to increase in proportion to exercise intensity (Kagaya & Homma, 1997) and reflect the
286 mBF response to exercise (Quaresima *et al.*, 2004). Therefore, the low-pressure occlusion must
287 be rapid (~0.5 s) and inflate immediately upon cessation of exercise. Secondly, the current study
288 was not able to collect ECG or individual hemoglobin concentrations, however it is encouraged
289 as time aligning the VO to cardiac cycles may increase reproducibility and individually sampled
290 hemoglobin concentrations will enhance the accuracy of absolute mBF rates. In addition,
291 synchronizing cuff inflation with ECG trace to occur at the same point within the cardiac cycle
292 may standardize the attenuation effects of the VO on mBF. Lastly, concurrent non-invasive
293 monitoring of additional parameters to assess the entire hemodynamic cascade may prove useful
294 for mechanistic and pathological determinants.

295 Ensuring high reproducibility of NIRS derived measurements within a single subject is a
296 critical step in the use of NIRS for clinical diagnosis. Our results have characterized reliability
297 for estimating relative changes immediate post exercise mBF and $m\dot{V}O_2$ across a wide range of
298 prevailing arterial inflows and O₂ consumption rates that can be used to estimate sample size and
299 incorporated into future experimental design. Using a standard protocol to compare

Local skeletal muscle blood flow and oxygen consumption assessment
300 measurements of mBF and $m\dot{V}O_2$ during exercise in trained, untrained, and diseased populations
301 will enhance our understanding of muscle physiology, mBF regulation, and disease pathogenesis.
302 More research is required to understand the effects of exercise and muscle contraction on: a) the
303 NIR light pathlength, b) changes in blood hemoglobin during exercise and its affect on mBF
304 measures, c) and the contribution of myoglobin to the NIR signal at various exercise stages for
305 the determination of absolute values of mBF and $m\dot{V}O_2$. Future research should compare
306 reliability and signal responses of continuous wave NIRS devices to other NIRS technologies, as
307 well as assess the reliability and validity of using occlusions during varying exercise modalities
308 and intensities compared to other leading techniques (Rådegran, 1999; Krix *et al.*, 2005;
309 Duerschmied *et al.*, 2006; Partovi *et al.*, 2012; Pollak *et al.*, 2012).

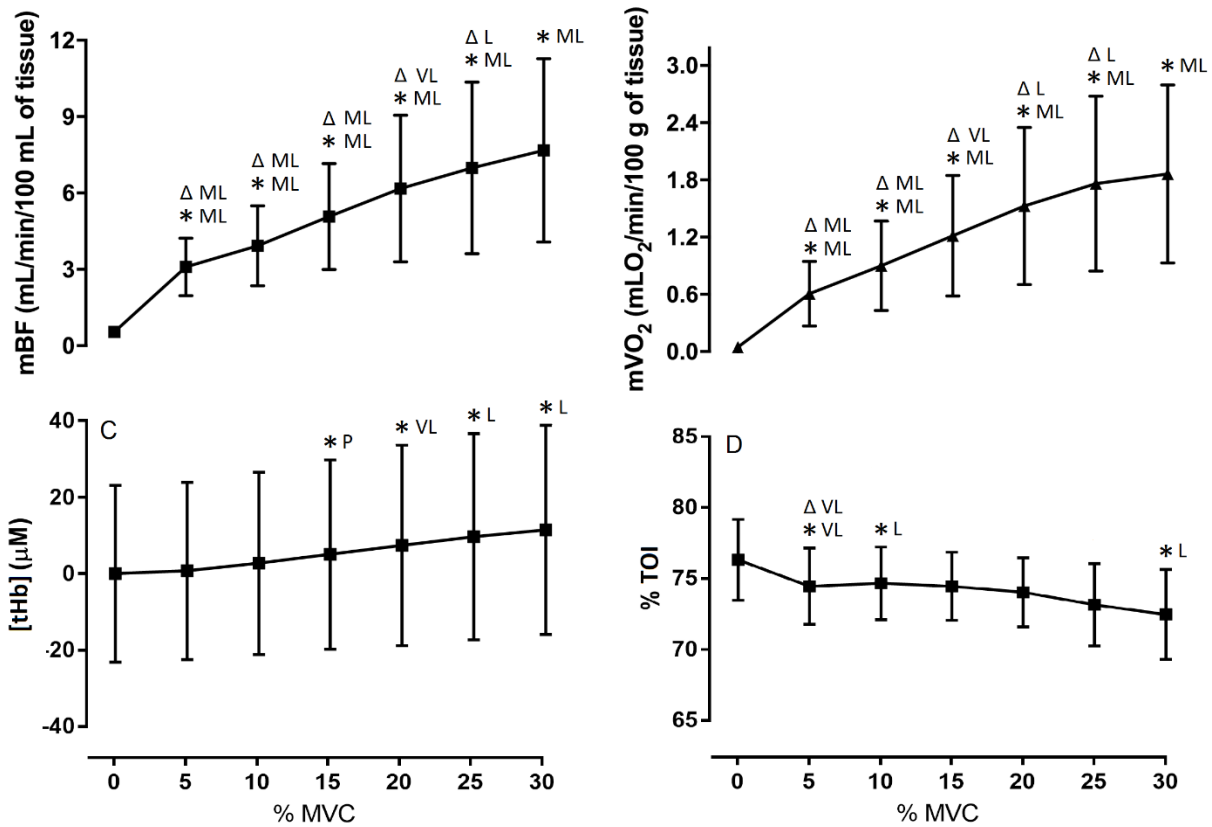
310 **Conclusion**

311 In summary, continuous wave NIRS devices can reliably assess mBF and $m\dot{V}O_2$ within
312 the microvasculature of the *vastus lateralis* during intermittent pauses from dynamic exercise in
313 healthy, physically active adults. The relative patterns of response for mBF, and $m\dot{V}O_2$ during
314 incremental exercise and mBF/ $m\dot{V}O_2$ ratio agree with other published results using similar
315 methodologies. Using NIRS to assess and characterize local parameters of skeletal muscle
316 hemodynamics and metabolism during rest and exercise opens new research paradigms for the
317 investigation of mBF regulation in health and disease with potential applications in clinical
318 diagnosis and therapeutic assessment.

319 **Figures and Tables**

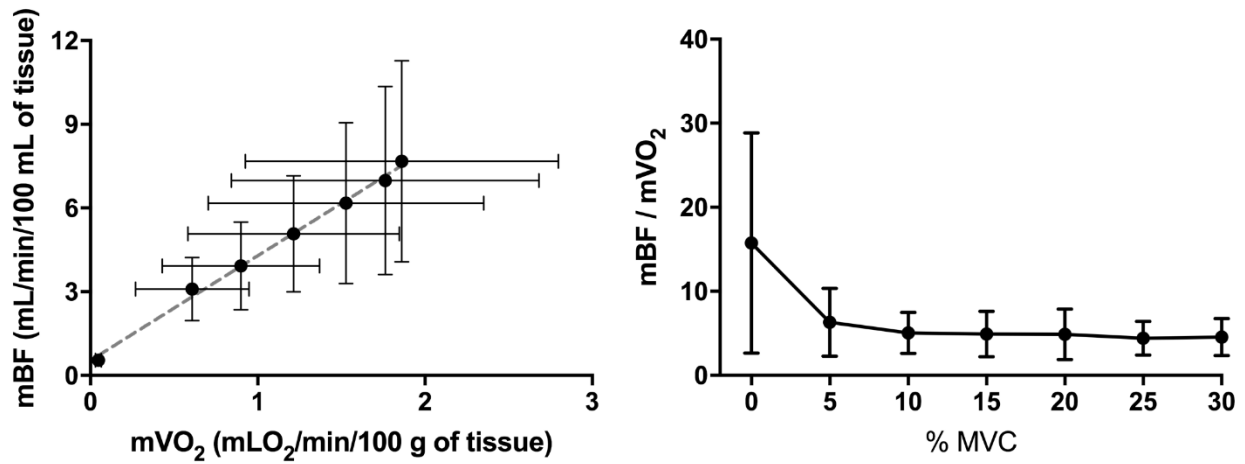
330 **Figure 1** *Experimental Protocol*. Representative example of NIRS signals (μM) collected from
 331 visits 2-4 showing the raw [tHb] (dark grey) and [HHb] (light grey) traces. The horizontal black
 332 lines above the x-axis denote the start and end of each intensity level (%MVC). Panel A shows
 333 the timeline (s) for one exercise intensity (5% MVC). After 3 min of knee extension exercise the
 334 cuff was rapidly inflated for 5-10 s for 4 venous occlusions (VO; 70-80 mmHg) and 2 arterial
 335 occlusions (AO; 250-300 mmHg) with 45 s of knee-extension exercise between occlusions for
 336 the assessment of mBF and m $\dot{V}\text{O}_2$, respectively. Zoom panels B and C show [tHb] and [HHb]
 337 signals for VO and AO, respectively, during rest. Zoom panels D and E show [tHb] and [HHb]
 338 signals for VO and AO, respectively, during exercise with three knee extensions on either side of
 339 occlusion. Black arrows denote the inflation and deflation of occlusion and the shaded gray area
 340 denotes the linear increase used in the assessment of mBF or m $\dot{V}\text{O}_2$

Local skeletal muscle blood flow and oxygen consumption assessment



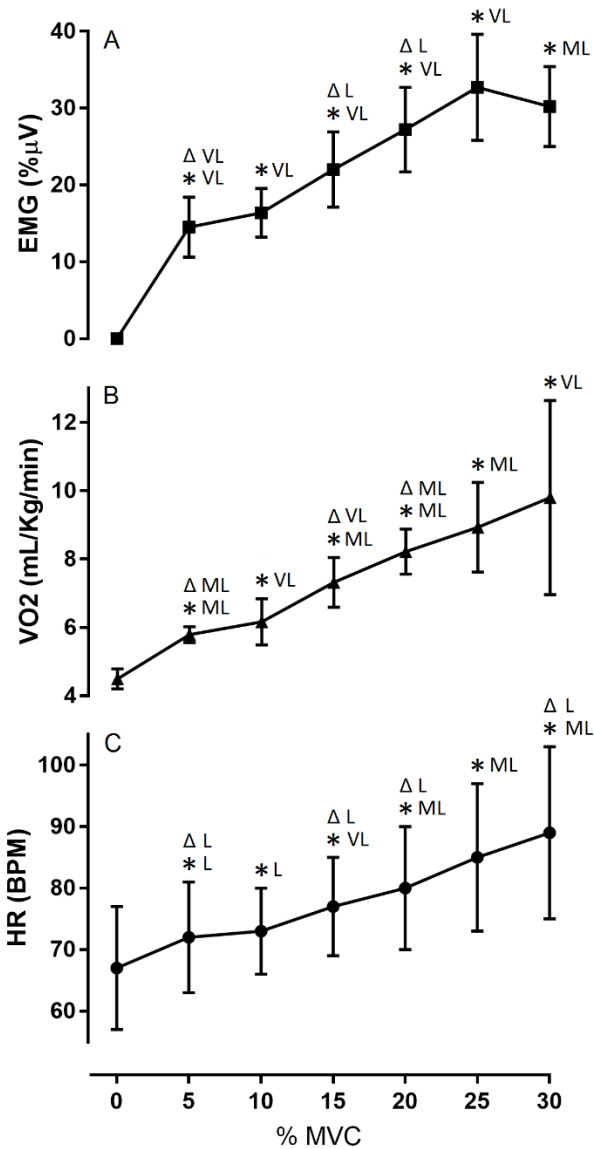
341

342 **Figure 2** The responses of all NIRS parameters over all exercise intensities. to increasing
 343 exercise intensity. Panels show (A) mBF, (B) m $\dot{V}O_2$, (C) relative perfusion, and (D) TSI%. Data
 344 are means and bars standard deviation. Workloads substantially greater (smallest effect) than
 345 resting or the previous workload are denoted with an asterisk (*), or a triangle (Δ), respectively.
 346 Statistical likelihoods are given next to the symbol as possible (P, 50-74.9%), likely (L, 75-
 347 94.9%), very likely (VL, 95-99.49%) and most likely (ML, 99.5-100%)



348

349 **Figure 3** The relationship between $m\dot{V}O_2$ and mBF over all exercise intensities. (A) mBF as a
 350 function of $m\dot{V}O_2$ with the regression line denoted by the dashed grey line given by the equation
 351 $y = 8.071x + 0.5482$; $R^2 = 0.9914$. (B) $m\dot{V}O_2/mBF$ ratio as a function of exercise intensity. Data
 352 are means and bars standard deviation



353

354 **Figure 4** Responses of EMG (top), $\dot{V}O_2$ (middle), and HR (bottom) to increasing exercise
 355 intensity. Data are means and bars standard deviation. Workloads substantially greater (smallest
 356 effect) than resting or the previous workload are denoted with an asterisk (*), likely (L,
 357 respectively. Chances are given next to symbol as possible (P, 50-74.9%), likely (L, 75-94.9%),
 358 very likely (VL, 95-99.49%) and most likely (ML, 99.5-100%)

359 **Table 1** Mean values and standard deviations for participant characteristics.

	Age	Height (m)	Weight (kg)	ATT (cm)	VL (cm)	VL Belly (cm)
Male	27.0	1.8	75.0	0.4	3.1	1.98
SD	7.0	0.0	9.6	0.2	0.41	0.31
Female	21.00	1.67	61.40	0.57	2.99	2.07
SD	4.00	0.05	0.42	0.16	0.47	0.26

Abbreviations: ATT, adipose tissue thickness; VL, vastus lateralis; VL Belly, distance from skin to the belly of the VL calculated as $ATT + 1/2 * VL$

360

361 **Table 2** Reliability of mBF and $m\dot{V}O_2$ for rest and all exercise intensities.

	Rest	5%	10%	15%	20%	25%	30%
<i>mBF</i>							
ICC	0.83	0.69	0.86	0.82	0.89	0.90	0.80
STE	0.45	0.59	0.41	0.46	0.37	0.35	0.48
CV (%)	14.6	31.0	21.4	24.8	20.9	20.2	30.4
SE (%)	5.5	7.7	8.9	9.0	10.0	10.2	10.1
<i>m$\dot{V}O_2$</i>							
ICC	0.58	0.92	0.93	0.91	0.91	0.96	0.96
STE	0.68	0.31	0.30	0.34	0.33	0.22	0.22
CV (%)	50.4	20.5	20.0	22.6	24.2	14.0	13.5
SE (%)	9.2	12.3	12.1	12.0	13.3	12.2	11.9
<i>Relative Perfusion – [tHb]</i>							
ICC	0.98	0.98	0.98	0.98	0.98	0.98	0.98
STE	0.18	0.16	0.17	0.17	0.15	0.17	0.16
CV (%)	4.0	3.7	4.0	4.1	3.8	4.1	3.8
SE (%)	4.5	4.6	4.6	4.7	4.9	4.9	4.9
<i>%TOI</i>							
ICC	0.71	0.87	0.86	0.75	0.70	0.76	0.78
STE	0.57	0.40	0.41	0.53	0.58	0.53	0.51
CV (%)	2.4	1.6	1.5	2.1	2.3	2.4	2.6
SE (%)	0.7	0.7	0.7	0.6	0.6	0.8	0.9

362 Abbreviations: ICC, intra-class correlation coefficient; STE, standardized typical error. The STE

363 magnitude thresholds are 0.1, 0.3, 0.6, 1, and 2 for small, moderate, large, very large, and

364 extremely large; %CV, coefficient of variation; %SE, Percentage for smallest effect.

365 **Additional Information:** No competing interests or conflicts of interest exist with any authors.

366 No external project fund was obtained.

367 **Supporting information:** Table 3. 90% Confidence limits for mean values of mBF, $m\dot{V}O_2$, and

368 tHb, and TOI% for rest & all exercise intensities.

369 **Author Contributions:**

370 A.A.L. and L.S. designed protocol with consult from J.F. and D.R.; A.A.L., G.A., W.L., and

371 B.N., recruited and collected data; A.A.L. analyzed the data; A.A.L., D.C., D.R., and L.S.

372 interpreted the data; A.A.L., G.A., W.L., B.N., drafted manuscript; A.A.L. prepared figures;

373 A.A.L, D.C., J.F, D.R., and L.S. edited and revised manuscript; A.A.L, D.R., and L.S. approved

374 the final version of manuscript.

375 **Acknowledgements**

376 We thank laboratory and other assistance from Shangari Venugopal, Brooke Price, Brandon

377 Woolley, Terrance Ryan, Kim Gaffney, Inge Ramakers, participants, and Roxanna J. Lucero.

378

379 **References**

- 380 Alkner BA, Tesch PA & Berg HE (2000). Quadriceps EMG/force relationship in knee extension and leg
381 press. *Medicine and science in sports and exercise* **32**, 459-463.
- 382
383 Andersen P, Adams RP, Sjogaard G, Thorboe A & Saltin B (1985). Dynamic knee extension as model for
384 study of isolated exercising muscle in humans. *Journal of Applied Physiology* **59**, 1647-1653.
- 385
386 Boushel R, Langberg H, Olesen J, Nowak M, Simonsen L, Bülow J & Kjær M (2000). Regional blood flow
387 during exercise in humans measured by near-infrared spectroscopy and indocyanine green.
388 *Journal of Applied Physiology* **89**, 1868-1878.
- 389
390 Casavola C, Paunescu LA, Fantini S & Gratton E (2000). Blood flow and oxygen consumption with near-
391 infrared spectroscopy and venous occlusion: spatial maps and the effect of time and pressure of
392 inflation. *Journal of biomedical optics* **5**, 269-276.
- 393
394 Casey DP, Curry TB & Joyner MJ (2008). Measuring muscle blood flow a key link between systemic and
395 regional metabolism. *Current opinion in clinical nutrition and metabolic care* **11**, 580.
- 396
397 Chance B, Dait MT, Zhang C, Hamaoka T & Hagerman F (1992). Recovery from exercise-induced
398 desaturation in the quadriceps muscles of elite competitive rowers. *American Journal of*
399 *Physiology-Cell Physiology* **262**, C766-C775.
- 400
401 Cross TJ & Sabapathy S (2015). The impact of venous occlusion per se on forearm muscle blood flow:
402 implications for the near-infrared spectroscopy venous occlusion technique. *Clinical physiology*
403 *and functional imaging*.
- 404
405 Duerschmied D, Olson L, Olschewski M, Rossknecht A, Freund G, Bode C & Hehrlein C (2006). Contrast
406 ultrasound perfusion imaging of lower extremities in peripheral arterial disease: a novel
407 diagnostic method. *European heart journal* **27**, 310-315.
- 408
409 Ferrari M, Muthalib M & Quaresima V (2011). The use of near-infrared spectroscopy in understanding
410 skeletal muscle physiology: recent developments. *Phil. Trans. R. Soc. A* **369**, 4577-4590.
- 411
412 Groebe K & Thews G (1990). Calculated intra-and extracellular PO₂ gradients in heavily working red
413 muscle. *American Journal of Physiology-Heart and Circulatory Physiology* **259**, H84-H92.
- 414
415 Hamaoka T, McCully KK, Niwayama M & Chance B (2011). The use of muscle near-infrared spectroscopy
416 in sport, health and medical sciences: recent developments. *Phil. Trans. R. Soc. A* **369**, 4591-
417 4604.
- 418

Local skeletal muscle blood flow and oxygen consumption assessment

- 419 Harper AJ, Ferreira LF, Lutjemeier BJ, Townsend DK & Barstow TJ (2006). Human femoral artery and
420 estimated muscle capillary blood flow kinetics following the onset of exercise. *Experimental*
421 *physiology* **91**, 661-671.
- 422
423 Hopkins W (2015). Spreadsheets for analysis of validity and reliability. *Sportscience* **19**, 36-42.
- 424
425 Hopkins W, Marshall S, Batterham A & Hanin J (2009). Progressive statistics for studies in sports
426 medicine and exercise science. *Medicine+ Science in Sports+ Exercise* **41**, 3.
- 427
428 Hopkins WG (2007). A spreadsheet for deriving a confidence interval, mechanistic inference and clinical
429 inference from a P value. *Sportscience* **11**, 16-21.
- 430
431 Ijichi S, Kusaka T, Isobe K, Okubo K, Kawada K, Namba M, Okada H, Nishida T, Imai T & Itoh S (2005).
432 Developmental changes of optical properties in neonates determined by near-infrared time-
433 resolved spectroscopy. *Pediatric research* **58**, 568-573.
- 434
435 Joyner MJ & Casey DP (2015). Regulation of increased blood flow (hyperemia) to muscles during
436 exercise: a hierarchy of competing physiological needs. *Physiological reviews* **95**, 549-601.
- 437
438 Kagaya A & Homma S (1997). Brachial arterial blood flow during static handgrip exercise of short
439 duration at varying intensities studied by a Doppler ultrasound method. *Acta physiologica*
440 *Scandinavica* **160**, 257-265.
- 441
442 Kalliokoski KK, Knuuti J & Nuutila P (2005). Relationship between muscle blood flow and oxygen uptake
443 during exercise in endurance-trained and untrained men. *Journal of Applied Physiology* **98**, 380-
444 383.
- 445
446 Komi PV & Tesch P (1979). EMG frequency spectrum, muscle structure, and fatigue during dynamic
447 contractions in man. *European Journal of Applied Physiology and Occupational Physiology* **42**,
448 41-50.
- 449
450 Krix M, Weber M-A, Krakowski-Roosen H, Huttner HB, Delorme S, Kauczor H-U & Hildebrandt W (2005).
451 Assessment of skeletal muscle perfusion using contrast-enhanced ultrasonography. *Journal of*
452 *Ultrasound in Medicine* **24**, 431-441.
- 453
454 Mancini DM, Bolinger L, Li H, Kendrick K, Chance B & Wilson JR (1994). Validation of near-infrared
455 spectroscopy in humans. *Journal of Applied Physiology* **77**, 2740-2747.
- 456
457 Miura H, McCully K, Nioka S & Chance B (2004). Relationship between muscle architectural features and
458 oxygenation status determined by near infrared device. *European Journal of Applied Physiology*
459 **91**, 273-278.
- 460

Local skeletal muscle blood flow and oxygen consumption assessment

- 461 Partovi S, Karimi S, Jacobi B, Schulte A-C, Aschwanden M, Zipp L, Lyo JK, Karmonik C, Müller-Eschner M &
462 Huegeli RW (2012). Clinical implications of skeletal muscle blood-oxygenation-level-dependent
463 (BOLD) MRI. *Magnetic Resonance Materials in Physics, Biology and Medicine* **25**, 251-261.
- 464
465 Paunescu LA, Casavola C, Franceschini M-A, Fantini S, Winter L, Kim J, Wood D & Gratton E (1999). Calf
466 muscle blood flow and oxygen consumption measured with near-infrared spectroscopy during
467 venous occlusion. In *BiOS'99 International Biomedical Optics Symposium*, pp. 317-323.
468 International Society for Optics and Photonics.
- 469
470 Pollak AW, Meyer CH, Epstein FH, Jiji RS, Hunter JR, DiMaria JM, Christopher JM & Kramer CM (2012).
471 Arterial Spin Labeling MR Imaging Reproducibly Measures Peak-Exercise Calf Muscle PerfusionA
472 Study in Patients With Peripheral Arterial Disease and Healthy Volunteers. *JACC: Cardiovascular*
473 *Imaging* **5**, 1224-1230.
- 474
475 Quaresima V, Ferrari M, Franceschini MA, Hoimes ML & Fantini S (2004). Spatial distribution of vastus
476 lateralis blood flow and oxyhemoglobin saturation measured at the end of isometric quadriceps
477 contraction by multichannel near-infrared spectroscopy. *Journal of biomedical optics* **9**, 413-420.
- 478
479 Rådegran G (1999). Limb and skeletal muscle blood flow measurements at rest and during exercise in
480 human subjects. *Proceedings of the Nutrition Society* **58**, 887-898.
- 481
482 Rådegran G, Blomstrand E & Saltin B (1999). Peak muscle perfusion and oxygen uptake in humans:
483 importance of precise estimates of muscle mass. *Journal of Applied Physiology* **87**, 2375-2380.
- 484
485 Rathbun S, Heath PJ & Whitsett T (2008). The venoarterial reflex. *Vascular Medicine* **13**, 315.
- 486
487 Richardson RS, Knight DR, Poole DC, Kurdak SS, Hogan MC, Grassi B & Wagner PD (1995). Determinants
488 of maximal exercise VO₂ during single leg knee-extensor exercise in humans. *American Journal*
489 *of Physiology-Heart and Circulatory Physiology* **268**, H1453-H1461.
- 490
491 Rudroff T, Weissman JA, Bucci M, Seppänen M, Kaskinoro K, Heinonen I & Kalliokoski KK (2014). Positron
492 emission tomography detects greater blood flow and less blood flow heterogeneity in the
493 exercising skeletal muscles of old compared with young men during fatiguing contractions. *The*
494 *Journal of physiology* **592**, 337-349.
- 495
496 Ryan TE, Erickson ML, Brizendine JT, Young H-J & McCully KK (2012). Noninvasive evaluation of skeletal
497 muscle mitochondrial capacity with near-infrared spectroscopy: correcting for blood volume
498 changes. *Journal of Applied Physiology* **113**, 175-183.
- 499
500 Southern WM, Ryan TE, Reynolds MA & McCully K (2013). Reproducibility of near-infrared spectroscopy
501 measurements of oxidative function and postexercise recovery kinetics in the medial
502 gastrocnemius muscle. *Applied Physiology, Nutrition, and Metabolism* **39**, 521-529.

Local skeletal muscle blood flow and oxygen consumption assessment

- 503
504 Van Beekvelt MC, Colier WN, Wevers RA & Van Engelen BG (2001). Performance of near-infrared
505 spectroscopy in measuring local O₂ consumption and blood flow in skeletal muscle. *Journal of*
506 *Applied Physiology* **90**, 511-519.
- 507
508 Vincent MA, Dawson D, Clark ADH, Lindner JR, Rattigan S, Clark MG & Barrett EJ (2002). Skeletal Muscle
509 Microvascular Recruitment by Physiological Hyperinsulinemia Precedes Increases in Total Blood
510 Flow. *Diabetes* **51**, 42-48.
- 511
512 Vogiatzis I, Habazettl H, Louvaris Z, Andrianopoulos V, Wagner H, Zakynthinos S & Wagner PD (2015). A
513 method for assessing heterogeneity of blood flow and metabolism in exercising normal human
514 muscle by near-infrared spectroscopy. *Journal of Applied Physiology* **118**, 783-793.
- 515
516 Vøllestad NK (1997). Measurement of human muscle fatigue. *Journal of neuroscience methods* **74**, 219-
517 227.
- 518
519 Watanabe K & Akima H (2011). Effect of knee joint angle on neuromuscular activation of the vastus
520 intermedius muscle during isometric contraction. *Scandinavian journal of medicine & science in*
521 *sports* **21**, e412-e420.
- 522
523 Whipp BJ & Ward SA (1982). Cardiopulmonary coupling during exercise. *Journal of Experimental Biology*
524 **100**, 175-193.